Model Based on Extracellular Potassium for Spontaneous Synchronous Activity in Developing Retinas

Burgi, Pierre-Yves; Grzywacz, Norberto M.

How to cite

BURGI, Pierre-Yves, GRZYWACZ, Norberto M. Model Based on Extracellular Potassium for Spontaneous Synchronous Activity in Developing Retinas. In: Neural computation, 1994, vol. 6, n° 5, p. 983–1004. doi: 10.1162/neco.1994.6.5.983

This publication URL: https://archive-ouverte.unige.ch//unige:17432
Publication DOI: 10.1162/neco.1994.6.5.983

Communicated by Raimond L. Winslow

Model Based on Extracellular Potassium for Spontaneous Synchronous Activity in Developing Retinas

Pierre-Yves Burgi
Norberto M. Grzywacz
The Smith-Kettlewell Eye Research Institute,
2232 Webster Street, San Francisco, CA 94115 USA

Waves of action-potential bursts propagate across the ganglion-cell surface of isolated developing retinas. It has been suggested that the rise of extracellular potassium concentration following a burst of action potentials in a cell may underlie these waves by depolarizing neighbor cells. This suggestion is sensible for developing tissues, since their glial system is immature. We tested whether this extracellular-potassium suggestion is feasible. For this purpose, we built a realistic biophysical model of the ganglion-cell layer of the developing retina. Simulations with this model show that increases of extracellular potassium are sufficiently high (about fourfold) to mediate the waves consistently with experimental physiological and pharmacological data. Even if another mechanism mediates the waves, these simulations indicate that extracellular potassium should significantly modulate the waves' properties.

1 Introduction

Recent multielectrode and optical-recording studies provided evidence that waves of bursts of activity propagate across the ganglion-cell surface (Meister *et al.* 1991) and inner plexiform layer (IPL) of the developing retina (Wong *et al.* 1992), correlating the activity of neighbor cells (Maffei and Galli-Resta 1990). Although the role of these waves has not yet been assessed, their possible contribution to forming layers of ocular dominance in the lateral geniculate nucleus (LGN) as well as in the refinement of a topographic map between retina and LGN has been hypothesized (Jeffery 1989; Meister *et al.* 1991).

What is the mechanism underlying these waves of bursts of activity? Because the waves propagate slowly (approximately 200 msec delay between neighbor ganglion cells in mammals), Meister *et al.* (1991) argued that it is unlikely that the waves are mediated by a fast synaptic mechanism or gap junctions. Further evidence against a gap-junction mechanism came from the preliminary evidence that octanol and dopamine, gap-junction blockers, have no significant effect on the correlation of

firing between neighbor ganglion cells (Sernagor and Grzywacz 1993a, 1994). Below we discuss more evidence that synaptic transmission is not likely to be the sole mechanism for wave propagation in mammals. Instead of synaptic and gap-junction mechanisms, Meister *et al.* (1991) hypothesized that an extracellular agent, such as K^+, might underlie the waves. Under this hypothesis, the ejection of K^+ by a cell's action potentials increases this ion's concentration in the extracellular space ($[K^+]_{out}$) and thus excites the neighbor cells. The significant reduction of correlation of firing between neighbor cells and the increase of interspike intervals when one blocks K^+ conductances with Cs^+ and tetraethylammonium (TEA) (Sernagor and Grzywacz 1993a) are consistent with (although do not prove) this hypothesis. Moreover, it is quite plausible that $[K^+]_{out}$ increases more in developing retinas than in adult retinas where waves of bursts do not occur (Masland 1977; Meister *et al.* 1991). The reason is that uptake of K^+ from extracellular space by Müller cells (see Dowling 1987 for a textbook treatment) might be slower in developing retinas (Sernagor and Grzywacz, personal communication). This immaturity of the retinal glial-cell system at early stages of development has already been reported (Rager 1979).

The aim of this paper is to build a realistic neural network model of the ganglion-cell layer of the developing retina to test whether modulation of $[K^+]_{out}$ could in principle mediate the waves (comparison of anatomical—McArdle *et al.* 1977; Maslim and Stone 1986; Horsburgh and Sefton 1987;—and physiological—Masland 1977; Maffei and Galli-Resta 1990; Meister *et al.* 1991—data shows that the correlated burst activity does not require other retinal cells). This model includes voltage- and calcium-dependent conductances, extracellular space, and synaptic inputs. Constraints to this model came from several studies in a variety of species during embryonic or postnatal periods. By using these constraints, we could build a model that is at least qualitatively consistent with the data from all species where correlated bursts have been studied. Above, we described speed-propagation and some pharmacological constraints. Other studies obtained values for the silent interval between bursts, rate of action potential inside bursts, and burst duration (Maffei and Galli-Resta 1990; Meister *et al.* 1991; Sernagor and Grzywacz, unpublished data). In turtle, the burst duration increases upon application of Cs^+ and TEA (Sernagor and Grzywacz 1993a). Furthermore, a dramatic reduction of activity with low Ca^{2+} and high Mg^{2+} (or in the presence of Co^{2+}, a calcium channel blocker) and the increase in activity with neostigmine (a cholinesterase inhibitor) suggested a synaptic role, at least partially cholinergic, for the propagation of waves in turtles (Sernagor and Grzywacz 1993a). A caveat is that such a cholinergic mechanism may not be mediated by conventional synapses (Zucker and Yazulla 1982; Lipton 1988). In any event, synaptic transmission is not likely to be the sole mechanism for wave propagation in mammals, as correlated activity occurs in the embryonic rat's retina (Maffei and Galli-Resta 1990),

despite the absence of conventional synapses in the IPL (Horsburgh and Sefton 1987). Similarly, in cat, waves appear on or before embryonic day 52 (E52) (Meister *et al.* 1991), whereas the first conventional synapses onto ganglion cells appear on E56 (Maslim and Stone 1986). Moreover, waves still exist under low Ca^{2+} without (Meister *et al.* 1991) and with (R. O. L. Wong, personal communication) high Mg^{2+}, and thus in the absence of conventional synaptic transmission. Although synapses might not be the main mechanism for wave propagation early in mammalian development, it has been suggested that they play a role in mammalian waves (Wong *et al.* 1992), perhaps later in development.

The new biophysical model is first presented in Section 2 and then described in mathematical detail in Section 3. The model's behavior has been studied by computer simulations of which wave-propagation results are presented in Section 4 (simulations of pharmacological results will be presented elsewhere—Burgi and Grzywacz 1994). The general discussion in Section 5 includes, among other things, a discussion on the choice of parameters and alternative models evaluated in terms of biological constraints. The material described in this paper appeared in abstract form elsewhere (Burgi and Grzywacz 1993a,b).

2 Description of the Model

In our model, K^+ is extruded from a ganglion-cell soma during action-potential activity. This extrusion increases $[K^+]_{out}$, leading to the depolarization of neighbor cells. Consequently, excitation propagates from cell to cell in a wave-like manner. The wave is prevented from propagating backwards by the activation of a K^+ conductance in the ganglion cells' dendrites. This K^+ conductance increases as intracellular Ca^{2+} builds up during a burst. Müller cells remove K^+ from the extracellular space to reset the retina.

Our goal was not to build a model that included all the intricacies of the developing retina, as, for example, all ionic channels and the detailed description of the dendrites. For instance, we did not use the detailed model for adult amphibian ganglion cells of Fohlmeister, Coleman, and Miller (1990), which uses five distinct channels in the soma alone (but no dendrite). This model predicts action-potential trains with high accuracy. But it is unclear whether this model's five channels exist in developing retinas and whether other channels are expressed in developing, but not adult retinas. Thus, rather than using an overly intricate model with elements unknown to exist in the developing retinas, we used a simple model that included only the elements necessary to account for the experimental behavior on correlated spontaneous activity. Nevertheless, we modeled these elements as realistically as possible to test the feasibility of whether ejection of K^+ into the extracellular space within the vicinity of ganglion cells may underlie the wave of bursts of action potentials.

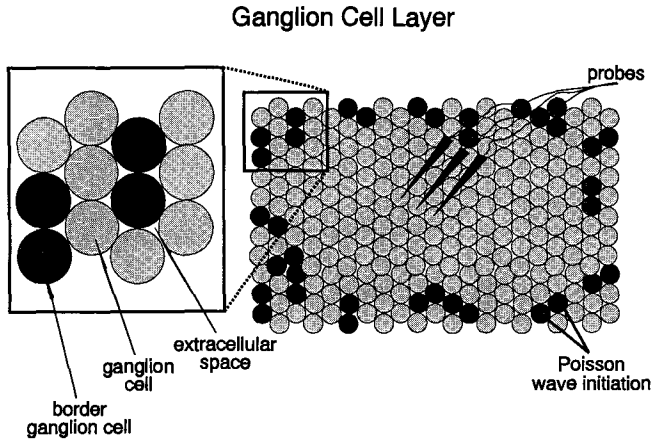

Figure 1: Model of ganglion cell layer. In this model, the cells are in a hexagonal arrangement. The circles delimit the area in which the cell is located, not the cell's size; the closest membrane-to-membrane distance between two neighbor cells is 12 μm. Wave initiation occurs at random border cells, shown in dark gray, where an external current is injected at times randomly drawn from a Poisson distribution. The three "electrodes" show cells whose spike activity is presented in Figure 2. Excitation propagates from cell to cell via extracellular K^+.

We built a hexagonal-geometry network of ganglion cells (Fig. 1), whose somas had Hodgkin–Huxley-like Na^+ and K^+ conductances, besides leak conductance and capacitance. This network approximates one layer of the three-dimensional ganglion cell architecture. Such approximation assumes that during a wave's propagation $[K^+]_{out}$ is equal in all the layers and thus there is no diffusion of K^+ from layer to layer. The assumption would fail near the extreme layers where loss of K^+ would slow down wave propagation.

The mechanism used to prevent waves from propagating backward is a calcium-activated potassium conductance (g_{AHP}), known to be slowly activated and sensitive to intracellular calcium concentrations ($[Ca^{2+}]_{in}$) in the range of 0.1–1 μM (Blatz and Magleby 1986). (This range of concentrations has been observed in dendrites of nerve cells—Regehr *et al.* 1989.) Support for such a mechanism comes from the elongation in burst duration during application of Cs^+ and TEA (Sernagor and Grzywacz 1993a) and by the elevation of $[Ca^{2+}]_{in}$ during a burst (Wong *et al.* 1992). However, neither the effect of Cs^+ and TEA nor the elevation

of $[Ca^{2+}]_{in}$ is direct evidence to g_{AHP}. Furthermore, only few papers reported the presence of calcium-activated potassium currents in ganglion cells (Lukasiewicz and Werblin 1988; Fohlmeister *et al.* 1990). Therefore, our confidence in the role of g_{AHP} in waves is small. We only used this conductance because its slow kinetics is consistent with the long interval between bursts. Instead, other slow conductances might mediate bursts' stoppage. In a subsequent paper (Burgi and Grzywacz 1994) modeling the effects of various pharmacological agents, we will address the likelihood of a calcium-dependent potassium conductance. In our model, Ca^{2+} entrance into the intracellular space is mediated through a fast Ca^{2+} conductance (g_{Ca}), activated by cell depolarization (Borg-Graham 1991). This Ca^{2+}-dependent K^+ conductance mechanism is also consistent with the effects of neostigmine, as an increase in cell's excitability by this drug should shorten the interspike interval, resulting in a faster increase in $[Ca^{2+}]_{in}$ and, thus, a shorter burst duration.

Using the same substance (K^+) for mediating excitation and inhibition may appear contradictory. We solved this contradiction by spatially separating the two processes. Ejection of K^+ resulting from depolarization of the cell is confined to the extracellular space around the soma, whereas ejection of K^+ resulting from g_{AHP} (and the associated Ca^{2+} conductance) occurs around the dendrite. At present, there is no evidence for the confinement of AHP and Ca^{2+} conductances to the dendrite. Exploratory computer simulations showed that if the K^+ ejected from the soma were to affect the reversal potential of g_{AHP}, then it would be harder, although still possible under limited conditions, to stop the bursts. This result provides a computational justification for our choice of the confinement of AHP and Ca^{2+} conductances to the dendrite.

Finally, the dendrite also receives an excitatory synaptic input (at least partially cholinergic) from amacrine cells to account for the low Ca^{2+} (or high Co^{2+}) and neostigmine effects in turtles (Sernagor and Grzywacz 1993a). (This input may not involve conventional synapses—Zucker and Yazulla 1982; Lipton 1988.) Although the model uses only one type of synapse, it is conceivable that other synapses, including possibly inhibitory ones, modulate the activity in the IPL. Hence, a limitation of our model may be the exclusion of other synapses involved directly or indirectly in the modulation of the waves' properties.

3 Methods

Each ganglion cell was modeled using two compartments, representing the dendrite and soma, connected by an axial conductance. Action potentials at the soma were determined by integrating the general membrane equation

$$C\frac{dV(t)}{dt} = -(I_{axial} + I_{Na} + I_K + I_{lK} + I_{l\neg K} + I_{border}) \tag{3.1}$$

where V is somatic voltage, C is membrane capacitance, I_{axial} is axial current flowing from the dendrite, I_{Na} and I_K are currents generated by the Na^+ and K^+ voltage-dependent conductances respectively, I_{lK} is the portion of the soma's leak current dependent on K^+, I_{l-K} is the portion of the soma's leak current not dependent on K^+, and I_{border} is a current injected into cells situated at the retinal border to initiate a wave (see below). The currents I_{Na} and I_K were determined by using a minimal biophysical model that condenses Hodgkin–Huxley equations (Av-Ron *et al.* 1991—see Appendix).

Current I_{axial} was given by the contribution of the conductances and Nernst potentials at the dendrite. After eliminating the dendritic voltage from the Kirchhoff equations, one gets

$$I_{axial} = \frac{\bar{g}_{axial}}{g_t + \bar{g}_{axial}} \sum_j (V - E_j) g_j + I_{syn} \tag{3.2}$$

where I_{syn} is (constant) synaptic current and $g_t = \sum_j g_j = g_{AHP} + g_{Ca} + g_d$, where g_{AHP} is calcium-dependent potassium conductance, g_{Ca} is transient voltage-dependent Ca^{2+} conductance, and g_d is leak membrane conductance at the dendrite. (The assumption of constant synaptic current may be a limitation of the model, as introduction of stochastic current might modulate some of the bursts' properties.) The g_{AHP} was expressed as a function of the fraction of a gating particle in the open state $\omega(t)$ as follows:

$$g_{AHP}(t) = \bar{g}_{AHP}\, \omega(t) \tag{3.3}$$

where $\bar{g}_{AHP}$ is maximal conductance. The differential equation for ω, according to the forward and backward rate constants (α and β, respectively), was (Borg-Graham 1991)

$$\dot{\omega}(t) = \alpha[1 - \omega(t)][Ca^{2+}]_{in}^3 - \beta\omega(t) \tag{3.4}$$

which means that the binding of three calcium ions is required to reach the open state. Variations in $[Ca^{2+}]_{in}$ as a function of calcium current I_{Ca} were described by the differential equation

$$\frac{d[Ca^{2+}]_{in}}{dt} = \frac{-I_{Ca}(t)}{2Fv_d} + \frac{1}{\tau_{Ca}}([Ca^{2+}]_{rest} - [Ca^{2+}]_{in}) \tag{3.5}$$

where F is the Faraday constant, the factor of 2 is for Ca^{2+} valence, v_d is dendritic volume, τ_{Ca} is a decay time constant, and $[Ca^{2+}]_{rest}$ is resting concentration in the dendrite. The calcium current that flows into the dendrite (negative by convention) was determined by using a two-state gate model (Borg-Graham 1991), which is described in the Appendix.

Extracellular K^+ is critical for the wave propagation in the model. This ion's extracellular concentration was considered homogeneous within the extracellular space between every three ganglion cells, that is, we neglected diffusion within each such spaces. We justify this simplification

because cell body surfaces are separated by approximately 10 μm (Meister *et al.* 1991) and K^+ ions diffuse in a three-dimensional aqueous medium over this distance in about 8 msec (Hille 1984—21 msec if one takes into account the tortuosity due to extracellular matrix, Nicholson *et al.* 1979). This period is much shorter than the time a wave takes to go from one ganglion cell to the next (approximately 200 msec—Meister *et al.* 1991).

We modeled active uptake of K^+ from the extracellular space by retinal Müller cells (Karwoski and Proenza 1980) by the following second-order removal differential equation:

$$\frac{d[K^+]_{out}}{dt} = \frac{I_K(t)}{Fv_0} - \frac{[K^+]_{out}}{\tau_K} - \kappa_K[K^+]^2_{out} + \frac{[K^+]_{rest}}{\tau_K} + \kappa_K[K^+]^2_{rest} \tag{3.6}$$

where v_0 is extracellular volume between every three cells, I_K is potassium current that flows into each of the six extracellular spaces surrounding the soma (except at the retinal border where K^+ flowing outward from the retina is assumed to be dissipated and not to contribute to the waves), τ_K is a decay time constant, κ_K is a constant, and $[K^+]_{rest}$ is resting extracellular potassium concentration. Evidence that K^+ uptake may be present concomitantly with waves of action potentials in developing retinas comes from recordings of b-waves in the turtle's electroretinogram (Sernagor and Grzywacz, unpublished data).

Variations in $[K^+]_{out}$ change the Nernst potential E_K, which affects the delayed rectifier current (I_K) and the portion of soma leak current (I_{lK}) that is dependent on K^+. Expression of the total soma leak current $I_l = I_{lK} + I_{l\neg K}$ as a function of E_K is given by

$$I_l = \bar{g}_l \left(V - \frac{E_K \bar{g}_{lK} + E_{l\neg K} \bar{g}_{l\neg K}}{\bar{g}_l} \right) \tag{3.7}$$

where $\bar{g}_l = \bar{g}_{lK} + \bar{g}_{l\neg K}$, and $\bar{g}_{lK}$ and $\bar{g}_{l\neg K}$ refer to the leak conductances whose Nernst potentials are K^+ dependent and independent, respectively.

A limitation in building our model is that no information is currently available on how waves begin. We assumed that cells are more excitable near the retinal border. In normal physiological conditions, this is probable, as neurogenesis occurs at the border (Polley *et al.* 1989), creating cells with small somata, and small or no dendrites, and thus cells that have high input resistance. Moreover, in experimental conditions, possible cuttings of dendritic trees at the border would depolarize cells. Therefore, we modeled border cells by reducing by half the dendritic volume and conductances. Waves were initiated by injecting a current I_{border} over a period of time T_{border} into a randomly chosen border-cell pair at times determined by a Poisson distribution.

A numerical method based on exponential prediction (as described in Ekeberg *et al.* 1991) was used to solve all differential equations. The computer simulations were performed on a SUN SPARC 2 using an object oriented language (C++). A network composed of 241 ganglion cells was simulated over a period of 200 sec. Over this period of time, the average

spike frequency, $[K^+]_{out}$, and the I_{AHP} current were recorded in all cells over successive 0.5 sec intervals. Furthermore, $[K^+]_{out}$, I_{AHP}, and soma potential were also recorded over successive 0.2 msec intervals for three neighbor cells situated in the middle of the network (shown in Fig. 1). The parameters used in the present simulations appear in the Appendix. Other simulations with a wide range of parameters and networks up to 1921 cells were also performed for exploratory purposes, obtaining results similar to those reported in this paper.

4 Results

The activity of single cells during wave propagation is shown in Figure 2. Figure 2A shows the burst activity of three neighbor cells resulting from seven sweeping waves. Although the activity of these three cells is correlated, the firing order can change from one burst to the next as the waves can start at different locations. This is apparent when comparing for instance the activity resulting from the first and second waves. The first wave hits the upper-trace cell first, then propagates to the middle-trace cell, and finally reaches the bottom-trace cell. The second wave hits these cells in reversed order. Moreover, because of differing propagation directions, the delay separating the activation of two neighbor cells can vary. The trace with extended time scale in Figure 2B shows individual spikes, within a burst resulting from the first wave, whose front propagated almost perpendicularly to the line connecting the three cells. This case yielded a delay from cell to cell of about 500 msec in our model. This speed is about a factor of 2.5 lower than that observed in cat and ferret (Meister *et al.* 1991). This discrepancy could be due to our choice of parameters to fit bursts' properties in the turtle retina. This cold-blooded tissue is less excitable than mammalian retinas, resulting in slower interspike intervals and thus, in our model, slower waves.

Variations of the interspike interval within a burst can also be seen in Figure 2B. The initial decrease in this interval is explained by the depolarization resulting from the ejection of K^+ from neighbor cells. This depolarization is apparent as an approximately 8 mV envelope on which the action potentials ride. Triggering of I_{AHP}-mediated self-inhibition by calcium accumulation counteracts this positive feedback, making the interspike interval increase again until the cell stops firing. (Despite the K^+-dependent inhibition at the end of the bursts, the voltage is not hyperpolarized, because the high $[K^+]_{out}$ causes compensatory depolarization.) Overall, with the present simulation parameters, the average interspike interval and burst duration were 190 and 2300 msec, respectively. These values are well within the experimentally observed range.

The interplay between $[K^+]_{out}$, firing frequency, and AHP current is illustrated in Figure 3. In this figure, the activity of a cell situated in the center of the network, and the variations in K^+ concentration of an

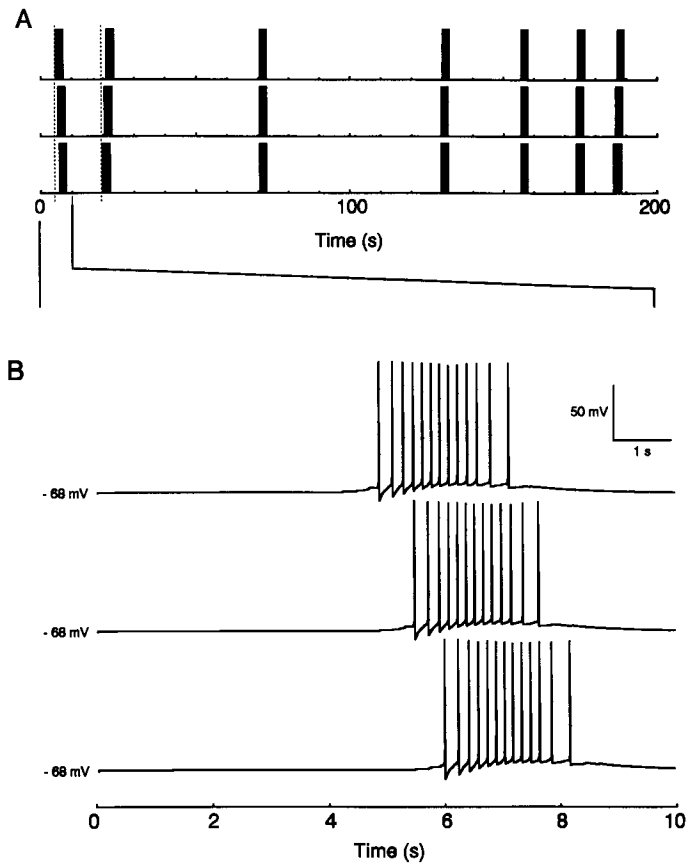

Figure 2: Bursts of action potentials. (A) The activity of three cells situated in the middle of the network, as shown in Figure 1, is plotted over a 200-sec period. Spikes, represented by individual lines, cannot be dissociated because of the low temporal resolution used in this figure. Although temporally correlated, the bursts do not start at the same time (emphasized by dashed line) because of the waves' directionality. (B) Action potentials from 0 to 10 sec expanded along the time axis to show time courses of individual spikes. Extracellular K^+ causes about 8 mV depolarization, on which the spikes ride on.

associated individual extracellular space are shown. The arrival of a wave causes the elevation of $[K^+]_{out}$. At a level of about 4.7 mM, the cell becomes so depolarized that a spike is generated. This spike, and the following ones, contribute to further $[K^+]_{out}$ elevation, which can be about

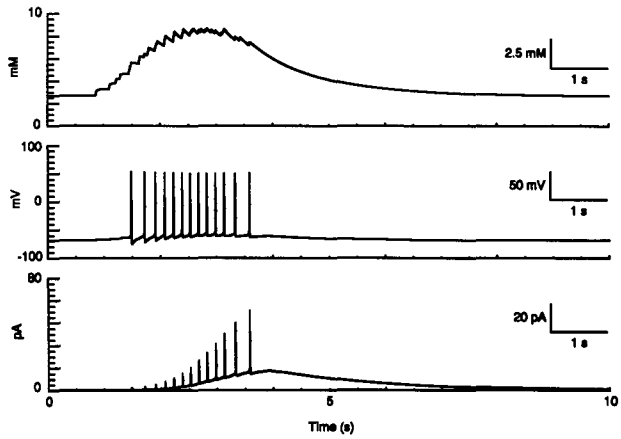

Figure 3: Time course of variables associated with a burst. Top trace shows the accumulation of K^+ that excites the cell whose membrane voltage is shown in the middle trace. Bottom trace shows the AHP current that is caused by membrane depolarization and that eventually inhibits the cell.

4-fold (from 2.6 to about 10 m*M*). The level of K^+ fluctuates rapidly, since it is increased by action potentials from the three neighbor cells surrounding the extracellular space where the measurement is made. At the same time, due to Ca^{2+} spikes (apparent in the I_{AHP} trace as transient spikes), the intracellular Ca^{2+} concentration starts building up. This rise in $[Ca^{2+}]_{in}$ activates the AHP conductance, which exerts a significant inhibitory effect on the cell's activity after a period of about 1.5 sec (visible in this figure as an elongation in the interspike interval). Once the inhibition is strong enough to stop the burst, $[K^+]_{out}$ enters a period of slow decrease. The slow I_{AHP} decay imposes a refractory period during which new waves are prevented from propagating. The long tails of I_{AHP} and $[K^+]_{out}$ are due to the relatively sluggish process of removal of Ca^{2+} and K^+ from intracellular and extracellular spaces, respectively.

The overall spatiotemporal pattern of the network activity corresponding to the first wave is presented in Figure 4 where $[K^+]_{out}$, average spike frequency (in 500 msec windows), and AHP current are shown over successive 1 sec for a period of 15 sec. The wave, triggered in the left bottom corner of the network, started propagating with a circular wave front. After the front reached the upper border of the network, the wave

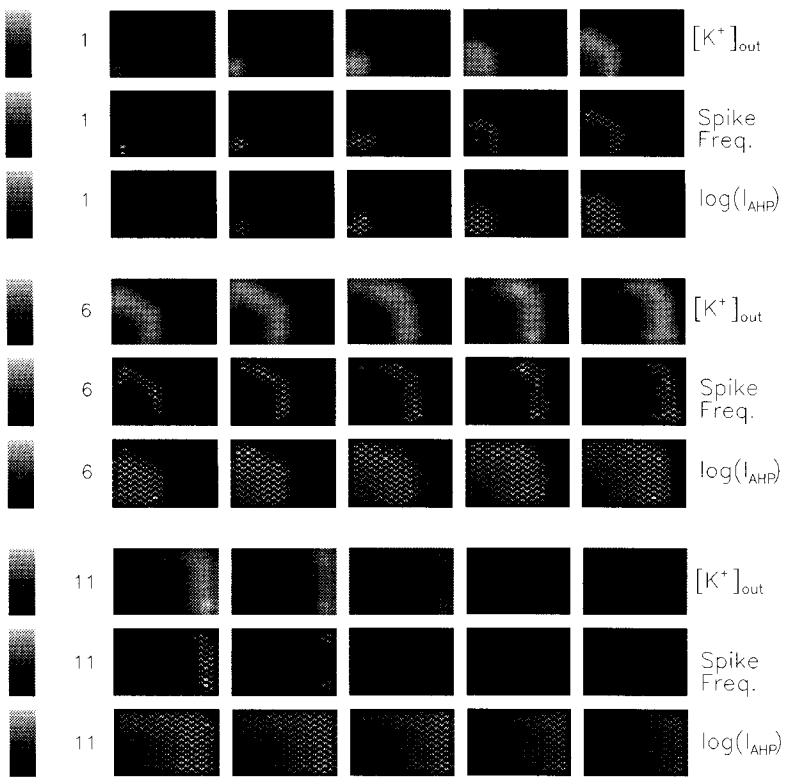

Figure 4: Spatiotemporal evolution of a wave. This wave swept through a network composed of 241 ganglion cells (Fig. 1). Successive frames show $[K^+]_{out}$ (top row), average firing rate (middle row), and logarithm of I_{AHP} (lower row) over successive 1 sec intervals covering the time interval from 1 to 15 sec; the serial number of the first frame of each row is indicated in the left column. Gray level scale is shown on the left and corresponds to the ranges 0–10 m*M* for $[K^+]_{out}$, 0–10 Hz for firing rate, and log(0.1)–log(35) pA for I_{AHP}. The $[K^+]_{out}$ wave precedes (causes) the action-potential firing wave, which in turn precedes (is terminated by) the AHP wave.

front became linear because of higher wave speed at the border cells due to their higher excitability. The degree of linearization is probably much higher than what one would predict for the real retina, since the number of cells in our simulations is relatively small, making the wave front more sensitive to border effects. These results suggest what would happen to

the wave front if waves began in the center of the retina. The wave front would be circular until it reached the borders. Spatial anisotropies due to the refractory periods from previous waves would rarely affect the wave front, because the interwave interval is very long. Therefore, the simulation variables would be essentially reset from wave to wave.

Also visible in this figure is the wave order: extracellular potassium wave leads the spike frequency wave (indicating that potassium triggers excitation), whereas the AHP wave lags spike frequency (indicating the refractory role of the calcium-dependent potassium conductances).

5 Discussion

5.1 Extracellular Potassium. Computer simulations of our biophysical model show that the propagation of waves of bursts of action potentials in the ganglion cell layer of developing retinas can in principle be explained by accumulation of K^+ in the extracellular space.

Are the model parameters determining $[K^+]_{out}$ reasonable? This concentration depends on the somatic K^+ currents, extracellular volume, and mechanism for K^+ removal. The parameters for the Hodgkin–Huxley K^+ channels (as well as for all other channels) were adapted from those of other preparations, as they are not currently available for the embryonic retina, except for sodium channel in dissociated ganglion cells (Skaliora *et al.* 1993). In this adaptation, the total value of each conductance and capacitance has been reduced by 3-fold to take into account the small soma diameter of embryonic neurons (Ramoa *et al.* 1988) and their reduced channel density (McCormick and Prince 1987). The only exception was g_{Ca} for which dendritic values were not available and thus had to be adjusted to give $[Ca^{2+}]_{in}$ in the range of g_{AHP} operation. As such, these conductances and capacitance are reasonable.

To estimate the extracellular volume, we used an 8 μm soma diameter (Ramoa *et al.* 1988), which occupies a volume of 2.7×10^{-13} liters. What fraction of the total volume is extracellular space? In postnatal developing neocortex, the volume fraction was estimated to range between 20 and 40% according to the animal's age (Lehmenkühler *et al.* 1993). (In adult cerebellum, the extracellular volume fraction is in average 20%—Van Harreveld 1972; Nicholson *et al.* 1979). In our simulations, we used an extracellular volume fraction of 30%, a value in the middle of the cortical postnatal range. Let us assume that the volume occupied by the extracellular matrix and the Müller cells is negligible. (This assumption is validated, since gliogenesis appears to be the major factor in reduction of extracellular volume fraction during development—Lehmenkühler *et al.* 1993—and since Müller cells are not well developed at the stage when waves occur.) Hence, the volume is shared by ganglion cells and extracellular space. From the 30% fraction, one gets 1.16×10^{-13} liters for the extracellular space associated to one cell. Because the K^+ current is

ejected into 6 extracellular spaces in our model, the volume of each space is 1.9×10^{-14} liters.

Finally, parameters of K^+ removal must be considered. In the central nervous system of adult mammals, $[K^+]_{out}$ rarely rises above 4 m*M* under physiological conditions (Somjen 1979). Concentrations of 10 m*M* extracellular potassium and higher have been recorded in preparations following repetitive activity (Somjen 1979). To take into account the immaturity of the glial system in developing retinas and the repetitive action-potential activity during bursts, we allowed a conservative elevation in $[K^+]_{out}$ up to 10 m*M* in control condition. Also, it has been suggested that a possible mechanism for K^+ active uptake into glial cells is the Na^+–K^+-ATPase exchanger (Hertz 1990). The Na^+–K^+-ATPase exchanger requires two K^+ molecules and thus, consistently with our model (equation 3.6), has a second-order stoichiometry. (In exploratory simulations, removal of the second-order term resulted in such a large increase of $[K^+]_{out}$ that cells underwent inactivation.) An active uptake mechanism based on the Na^+–K^+-ATPase exchanger is consistent with studies on the cerebral cortex of rat during early postnatal development (Medzihradsky *et al.* 1972) where it has been shown that this exchanger in glial cells is immature during the initial stages of development.

How do the extracellular volume and K^+ removal change during development? There are no direct data on these issues for developing retinas. However, in rat neocortex the extracellular volume fraction appears to decrease during development possibly as a consequence of the emergence of glial cells (Lehmenkühler *et al.* 1993). Because in the retina, glial (Müller) cells also emerge relatively late in development (Polley *et al.* 1989), one might expect a similar reduction of extracellular volume fraction in the retina as in the neocortex. Reduction in volume would make a $[K^+]_{out}$ mechanism for waves more efficient. On the other hand, an increase in the number of mature Müller cells would tend to compensate for the effect of reduction of volume. If our model is correct, one should expect the effect of increased K^+ buffering by Müller cells to dominate the effect of change in extracellular volume, since waves disappear at later stages of development.

5.2 Possible Role of Waves in the Refinement of Topographic Maps. Synchronization is much more localized in developing retinas than in other tissues where bursty activity has been observed, such as in the pancreas (Santos *et al.* 1991), heart (Winfree 1990), and in aggregates of cultured cortical neurons (Murphy *et al.* 1992). The reason for this difference is probably qualitative, rather than quantitative: Because pharmacology performed on developing retinas of turtles (Sernagor and Grzywacz 1993a) suggested that gap junctions are not required to synchronize the activity of neighbor ganglion cells, we did not include such connections in our model. This is probably the main difference to previous models of cell synchronization in the heart and pancreas where coupling is appar-

ently done through gap junctions (Chay and Kang 1988; Sherman and Rinzel 1991; Winslow *et al.* 1993). In those models, coupling is so fast that a global synchronization of the network is reached, in the sense that all cells fire simultaneously at some point. This global synchronization contrasts to the locality of developing retinas where the slow propagation of the activity restricts synchronization to a small portion of the network.

Local synchronization is essential in developing retinas if its role is to refine a topographic map between retina and LGN (Jeffery 1989; Meister *et al.* 1991; Wong *et al.* 1993). Imagine that immature ganglion-cell axons sprout over a relatively large area and connect random LGN neurons (with a bell-shaped spatial distribution), forming a rough topographic map. Then, simultaneous activity in neighbor ganglion cells coupled to a Hebbian mechanism in the LGN would tend to reinforce connections to common, nearby LGN neurons, while weakening connections in the fringes of the axonal sprouting. This process would refine the receptive fields in LGN and, consequently, refine the topographic continuity of the retina-LGN map. The refinement would be limited by the wave's spread. Hence, if waves were too broad, causing global synchronization, there would be no topographic refinement.

5.3 Alternative Models. Our model and the models for other tissues emphasize two main requirements for waves: (1) local lateral excitation, which allows wave propagation and (2) inhibition, which prevents waves from propagating backward (refractory period).

Figure 5 displays three possible alternative mechanisms for inhibition. The first, self-inhibition (for example, via g_{AHP}), has been used in our and other models (Fig. 5A). The second is a neurotransmitter that is depleted or a receptor that is desensitized following strong activity (Fig. 5B). The third, feedforward inhibition, is a delayed lateral synaptic inhibition between neighbor units (Fig. 5C). We argue that the second alternative, namely depletion or desensitization, is unlikely to be the main refractory mechanism stopping the bursts in developing retinas. These mechanisms take place at synapses and thus require that lateral excitatory synapses mediate wave propagation. However, in mammals, correlated activity and waves have been recorded in retinas so young that they did not have synapses onto ganglion cells yet (Maslim and Stone 1986; Horsburgh and Sefton 1987; Maffei and Galli-Resta 1990; Meister *et al.* 1991). Furthermore, the requirement that lateral excitatory synapses mediate wave propagation raises serious difficulties to explain the Cs^+ and TEA result in turtle. Removing the inhibitory effect of K^+ would tend to increase excitation and prolong spikes, and thus should cause faster transmitter depletion or receptor desensitization. Hence, these inhibitory mechanisms would cause shorter burst duration, contrary to experimental evidence (Sernagor and Grzywacz 1993a). We argue that not only depletion and desensitization are unlikely but also feedforward inhibition (Fig. 5C). In mammals, the IPL synaptic circuitry is not developed

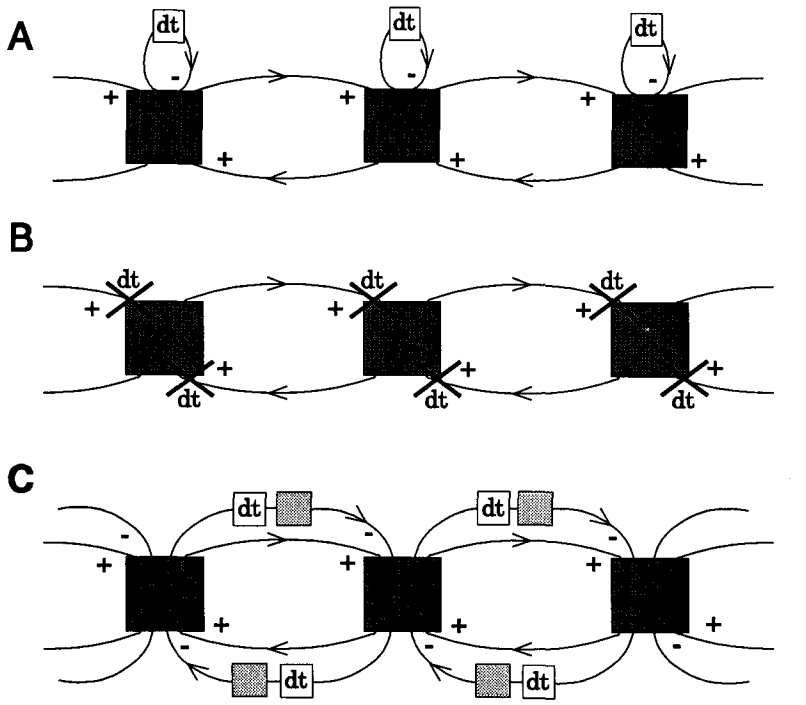

Figure 5: Three computational models for waves of activity. In all the models, there are excitatory (not necessarily synaptic) couplings between neighboring cells. Delayed activity suppression, critical to the waves' refractory period, can be accomplished by using (A) self-inhibition (for example, through I_{AHP}), where the cell's activity determines its own level of inhibition, (B) attenuation of excitatory synaptic transmission through transmitter depletion or receptor desensitization, or (C) feedforward connections through an inhibitory interneuron.

at the time where synchronous burst firing first occurs. In turtles, there is a serious time constraint, as synaptic inhibition onset would have to be at least as slow as the slowest burst duration, that is, about 20 sec (Sernagor and Grzywacz, unpublished data).

In our model, we chose $[K^+]_{out}$ to mediate lateral excitation, but two alternative mechanisms, gap junctions and synapses, cannot be completely ruled out. Although Sernagor and Grzywacz's (1993a, 1994) studies provide evidence against gap junctions, it is possible that the gap junction blockers used in these studies, namely octanol and dopamine, are not ap-

propriate in developing retinas. The evidence against the involvement of synapses as a mechanism for wave propagation in mammals is strong. Anatomical studies performed in postnatal rat show that IPL conventional synapses are first observed on postnatal day 11 (P11) (Horsburgh and Sefton 1987), whereas spontaneous synchronized discharges can be recorded before birth (Maffei and Galli-Resta 1990). Moreover, in cat, conventional synapses onto ganglion cells first appear on E56 (Maslim and Stone 1986), while waves have been recorded from an E52 retina (Meister *et al.* 1991). In cats and ferrets, activity and the synchronization remained (and even increased) under Ca^{2+}-free conditions (without—Meister *et al.* 1991—and with—R. O. L. Wong, personal communication—high Mg^{2+}) and, thus, presumably, without conventional synaptic transmission. (The increase in activity is perhaps due to a reduction of the Ca^{2+}-dependent K^+-mediated inhibition, a mechanism suggested by our model.) Finally, Meister *et al.* (1991) argued against fast synapses, because they must have a very slow integration time to account for the slow propagation between neighbor cells (approximately 200 msec in mammals—Meister *et al.* 1991). In view of the strong evidence against synaptic mediation of waves, the result of Wong *et al.* (1992) who found that waves activate both ganglion and amacrine cells of developing retinas is surprising. One way to interpret our model to explain this result is to postulate that K^+ waves simultaneously propagate across amacrine and ganglion cells. However, if this is the case, then the inhibitory mechanism preventing the waves from propagating backwards might not be I_{AHP}, since its effectiveness would be reduced by the increase in $[K^+]_{out}$. Another K^+-independent self-inhibition process might be used instead.

5.4 Synapses. In contrast to mammals, there is direct evidence in turtles for a role of synapses in correlated burst activity. Neostigmine, an anticholinesterase, increases burst activity, indicating release of acetylcholine (Ach) and the functionality of Ach receptors in the IPL (Sernagor and Grzywacz 1993a). In addition, there is a large reduction of activity in low Ca^{2+} and high Mg^{2+} (or in presence of Co^{2+}) (Sernagor and Grzywacz 1993a). Although Co^{2+} or neostigmine experiments have not as yet been performed in mammals, it is possible that results similar to those of turtles would be found at late stages of development. (As mentioned above, in early stages of mammalian development waves have been recorded in the absence of conventional synapses.)

The role of synapses might actually be to transmit excitation laterally to mediate propagation itself. Alternatively, our model suggests that the role of synapses might be of neuromodulation of speed or spatial spread of waves. A potential function of such neuromodulation could be the regulation of spatial interaction during development. For instance, increases in ganglion cell excitability due to strengthening of excitatory synapses might compensate for the decrease in $[K^+]_{out}$ resulting from the development of Müller cells, as it was discussed above.

Synapses might not only modulate wave propagation, but also might be modulated by it. Because of the Wong *et al.*'s (1992) evidence that at some point during development waves propagate simultaneously in the IPL and ganglion cells, waves might modify amacrine–ganglion synaptic strength in a Hebbian manner (Borg-Graham and Grzywacz 1992) to form the experimentally observed prenatal orientation selectivity of turtles (Sernagor and Grzywacz, 1993b) and pre-eye-opening directional selectivity of rabbits (Masland 1977). This idea is similar to that proposed by Linsker (1986) and Miller (1994) to explain the emergence of cortical orientational selectivity from random spontaneous activity.

6 Conclusions

Modulations in extracellular K^+ concentration might be sufficiently high to carry the spontaneous waves of action potentials in developing retinas. Even if another mechanism underlies the waves, these modulations are so large that they would affect the waves' properties. We argue that the refractory mechanism preventing the waves from propagating backward is unlikely to be neurotransmitter depletion, receptor desensitization, or feedforward synaptic inhibition. Rather, this mechanism might be self-inhibition, such as mediated by an AHP or another slow conductance. Finally, it is proposed that excitatory synapses might have a neuromodulatory role in the shaping of waves' properties.

Appendix

The condensed Hodgkin–Huxley equations at the soma for I_{Na} and I_K are described by a minimal cell model proposed by Av-Ron *et al.* (1991), whose equations are

$$I_{Na} = \bar{g}_{Na} m_\infty^3(V)(1 - W)(V - E_{Na}) \tag{A.1}$$

$$I_K = \bar{g}_K (W/s)^4 (V - E_K) \tag{A.2}$$

$$m_\infty(V) = \frac{1}{1 + \exp[-2a^{(m)}(V - V_{1/2}^{(m)})]} \tag{A.3}$$

$$\frac{dW}{dt} = \frac{W_\infty(V) - W}{\tau(V)} \tag{A.4}$$

$$W_\infty(V) = \frac{1}{1 + \exp[-2a^{(w)}(V - V_{1/2}^{(w)})]} \tag{A.5}$$

$$\tau(V) = \frac{1}{\bar{\lambda}\exp[a^{(w)}(V - V_{1/2}^{(w)})] + \bar{\lambda}\exp[-a^{(w)}(V - V_{1/2}^{(w)})]} \tag{A.6}$$

where $\bar{g}_{Na}$ and $\bar{g}_K$ are maximal conductances, E_{Na} and E_K are reversal potentials, and s, $a^{(m)}$, $V_{1/2}^{(m)}$, $a^{(w)}$, $V_{1/2}^{(w)}$, and $\bar{\lambda}$ are positive channel parameters.

Current I_{Ca} at the dendrite (given the dendritic membrane potential V_d), is described by a two-state gate model (Borg-Graham 1991):

$$I_{Ca} = \bar{g}_{Ca} y^2 (1 - w^4)(V_d - E_{Ca}) \tag{A.7}$$

where $\bar{g}_{Ca}$ is maximal membrane conductance, E_{Ca} is reversal potential, and the gating particles y and $1 - w$ represent activation and inactivation, respectively. The general equations for these gating particles (hereinbelow denoted by x) are given by

$$\frac{dx}{dt} = \frac{x_\infty - x}{\tau} \tag{A.8}$$

$$x_\infty = \frac{\alpha}{\alpha + \beta} \tag{A.9}$$

$$\tau = \frac{1}{\alpha + \beta} \tag{A.10}$$

$$\alpha = \alpha_0 \exp\left[\frac{-z\gamma}{K}(V - V_{1/2})\right] \tag{A.11}$$

$$\beta = \beta_0 \exp\left[\frac{z(1-\gamma)}{K}(V - V_{1/2})\right] \tag{A.12}$$

where V is the membrane potential, z, α_0, β_0, γ, and $V_{1/2}$ are parameters of the channel, and $K = 25$ mV at 20°C.

All parameters used in the simulations described in this paper are adapted from Yamada *et al.* (1989), Borg-Graham (1991), and Ekeberg *et al.* (1991). This adaptation takes into account the small size of the cells and relatively low channel density in immature neurons. For the synaptic current, its value is comparable to external currents injected into dissociated fetal retinal ganglion cells (Skaliora *et al.* 1993). The parameters are summarized in Tables 1 and 2. Table 1 describes parameters related to somatic and dendritic conductances. Table 2 describes parameters related to intra- and extracellular concentrations, as well as other miscellaneous parameters.

Acknowledgments

We thank Dr. Evelyne Sernagor for the many discussions during the course of this project. Also, we are grateful to Drs. Sernagor, Lyle Borg-Graham, and Markus Meister for their fruitful comments on this paper. This work was supported by a grant from the Swiss National Fund for Scientific Research (8220-37180) to P.-Y. B., by grants from the National Eye Institute (EY-08921) and Office of Naval Research (N00014-91-J-1280), and by an award from the Paul L. and Phyllis C. Wattis Foundation to N. M. G., and by a core grant from the National Eye Institute to Smith-Kettlewell (EY-06883).

Table 1: Somatic and Dendritic Conductance Parameters.

Soma	Leak	$\bar{g}_{lK} = 0.88$ nS, $\bar{g}_{l\neg K} = 0.12$ nS	
		$E_{l\neg K} = 88$ mV	
	Na	$\bar{g}_{Na} = 0.33$ μS	$a^{(w)} = 0.059$ mV^{-1}
		$E_{Na} = 55$ mV	$a^{(m)} = 0.047$ mV^{-1}
	K	$\bar{g}_K = 0.067$ μS,	$V_{1/2}^{(w)} = -57$ mV
		E_K = variable	$V_{1/2}^{(m)} = -34$ mV
		$s = 1.85$	$\bar{\lambda} = 2.9$ Hz
Dendrite	Leak	$\bar{g}_d = 1$ nS, $E_d = -70$ mV	
	Ca	$\bar{g}_{Ca} = 0.017$ nS, E_{Ca} = variable	
		State variable s	$\alpha_0 = 0.1$ ms^{-1}
			$\beta_0 = 0.1$ ms^{-1}, $\gamma = 0.5$
			$V_{1/2} = -24$ mV, $z = 4$
		State variable w	$\alpha_0 = 0.008$ ms^{-1}
			$\beta_0 = 0.008$ ms^{-1}, $\gamma = 0.2$
			$V_{1/2} = -35$ mV, $z = 12$
	AHP	$\bar{g}_{AHP} = 4$ nS, $E_{AHP} = -88$ mV	
		$\alpha = 2.0 \times 10^6$ ms^{-1} mM^{-3},	
		$\beta = 0.002$ ms^{-1}	

Table 2: Intracellular and Extracellular Concentration Parameters.

$[K^+]_{out}$	$[K^+]_{rest} = 2.6$ mM, $[K^+]_{in} = 100$ mM
	$v_o = 2.0 \times 10^{-14}$ liters, $\tau_K = 2.0$ sec,
	$\kappa_K = 5.0 \times 10^{-2}$ sec^{-1} mM^{-1}
$[Ca^{2+}]_{in}$	$[Ca^{2+}]_{rest} = 150$ nM, $[Ca^{2+}]_{out} = 4$ mM
	$v_d = 5.0 \times 10^{-14}$ liters, $\tau_{Ca} = 3.3$ sec
Miscellaneous	$I_{ext} = -25$ pA, $T_{border} = 250$ msec, $I_{syn} = -2$ pA
	$\bar{g}_{axial} = 0.03$ μS, $C = 3$ pF

References

Av-Ron, E., Parnas, H., and Segel, L. A. 1991. A minimal biophysical model for an excitable and oscillatory neuron. *Biol. Cybern.* **65**, 487–500.

Blatz, A. L., and Magleby, K. L. 1986. Single apamin-blocked Ca-activated K^+ channels of small conductance in cultured rat skeletal muscle. *Nature (London)* **323**, 718–720.

Borg-Graham, L. J. 1991. Modelling the non-linear conductances of excitable membranes. In *Cellular and Molecular Neurobiology: A Practical Approach,*

H. Wheal and J. Chad, eds., pp. 247–275. Oxford University Press, Oxford, UK.

Borg-Graham, L. J., and Grzywacz, N. M. 1992. A model of the directional selectivity circuit in retina: Transformations by neurons singly and in concert. In *Single Neuron Computation*, T. McKenna, J. Davis, and S. F. Zornetzer, eds., pp. 347–375. Academic Press, Boston.

Burgi, P.-Y., and Grzywacz, N. M. 1993a. A biophysical model of synchronous bursts of activity in ganglion cells of the developing retina. *Invest. Ophthalmol. Vis. Sci.* **34**, 1155.

Burgi, P.-Y., and Grzywacz, N. M. 1993b. Model for initiation and propagation of waves of action potentials in developing retinas. *Neurosci. Abstr.* **19**, 239.

Burgi, P.-Y., and Grzywacz, N. M. 1994. Model for the pharmacological basis of spontaneous synchronous activity in developing retinas. *J. Neurosci.*, in press.

Chay, T. R., and Kang, H. S. 1988. Role of single-channel stochastic noise on bursting clusters of pancreatic β-cells. *Biophys. J.* **54**, 427–435.

Dowling, J. E. 1987. *The Retina*. Harvard University Press, Cambridge, MA.

Ekeberg, Ö., Wallén, P., Lansner, A., Tråvén, H., Brodin, L., and Grillner, S. 1991. A computer based model for realistic simulations of neural networks. *Biol. Cybern.* **65**, 81–90.

Fohlmeister, J. F., Coleman, P. A., and Miller, R. F. 1990. Modeling the repetitive firing of retinal ganglion cells. *Brain Res.* **510**, 343–345.

Hertz, L. 1990. Regulation of potassium homeostasis by glial cells. In *Differentiation and Functions of Glial Cells*, pp. 225–234. A. R. Liss, New York.

Hille, B. 1984. *Ionic Channels of Excitable Membranes*. Sinauer, Sunderland, MA.

Horsburgh, G. M., and Sefton, A. J. 1987. Cellular degeneration and synaptogenesis in the developing retina of the rat. *J. Comp. Neurol.* **263**, 553–566.

Jeffery, G. 1989. Shifting retinal maps in the development of the lateral geniculate nucleus. *Dev. Brain Res.* **46**, 187–196.

Karwoski, C. J., and Proenza, L. M. 1980. Neurons, potassium, and glia in proximal retina of Necturus. *J. Gen. Physiol.* **75**, 141–162.

Lehmenkühler, A., Syková, E., Svoboda, J., and Nicholson, C. 1993. Extracellular space parameters in the rat neocortex and subcortical white matter during postnatal development determined by diffusion analysis. *Neuroscience* **55**, 339–351.

Linsker, R. 1986. From basic network principles to neural architecture: Emergence of orientation-selective cells. *Proc. Natl. Acad. Sci. U.S.A.* **83**, 8390–8394.

Lipton, S. A. 1988. Spontaneous release of acetylcholine affects the physiological nicotinic responses of rat retinal ganglion cells in culture. *J. Neurosci.* **8**, 3857–3868.

Lukasiewicz, P., and Werblin, F. 1988. A slowly inactivating potassium current truncates spike activity in ganglion cells of the tiger salamander retina. *J. Neurosci.* **8**, 4470–4481.

McArdle, C. B., Dowling, J. E., and Masland, R. H. 1977. Development of outer segments and synapses in the rabbit retina. *J. Comp. Neurol.* **175**, 253–274.

McCormick, D. A., and Prince, D. A. 1987. Post-natal development of elec-

trophysiological properties of rat cerebral cortical pyramidal neurones. *J. Physiol. (London)* **393**, 743–762.

Maffei, L., and Galli-Resta, L. 1990. Correlation in the discharges of neighboring rat retinal ganglion cells during prenatal life. *Proc. Natl. Acad. Sci. U.S.A.* **87**, 2861–2864.

Masland, R. H. 1977. Maturation of function in the developing rabbit retina. *J. Comp. Neurol.* **175**, 275–286.

Maslim, J., and Stone, J. 1986. Synaptogenesis in the retina of the cat. *Brain Res.* **373**, 35–48.

Medzihradsky, F., Sellinger, O. Z., Nandhasri, P. S., and Santiago, J. C. 1972. ATPase activity in glial cells and in neuronal perikarya of rat cerebral cortex during early postnatal development. *J. Neurochem.* **19**, 543–545.

Meister, M., Wong, R. O. L., Baylor, D. A., and Shatz, C. J. 1991. Synchronous bursts of action potentials in ganglion cells of the developing mammalian retina. *Science* **252**, 939–943.

Miller, K. D. 1994. A model for the development of simple cell receptive fields and the ordered arrangement of orientation columns through activity-dependent competition between ON- and OFF-center inputs. *J. Neurosci.* **14**, 409–441.

Murphy, T. H., Blatter, L. A., Wier, W. G., and Baraban, J. M. 1992. Spontaneous synchronous synaptic calcium transients in cultured cortical neurons. *J. Neurosci.* **12**, 4834–4845.

Nicholson, C., Phillips, J. M., and Gardner-Medwin, A. R. 1979. Diffusion from an iontophoretic point source in the brain: Role of tortuosity and volume fraction. *Brain Res.* **169**, 580–584.

Polley, E. H., Zimmerman, R. P., and Fortney, R. L. 1989. Neurogenesis and maturation of cell morphology in the development of the mammalian retina. In *Development of the Vertebrate Retina*, B. L. Finlay and D. R. Sengelaub, eds., pp. 3–29. Plenum Press, New York.

Rager, G. 1979. The cellular origin of the b-wave in the electroretinogram—a developmental approach. *J. Comp. Neurol.* **188**, 225–244.

Ramoa, A. S., Campbell, G., and Shatz, C. J. 1988. Dendritic growth and remodelling of cat retinal ganglion cells during fetal and postnatal development. *J. Neurosci.* **8**, 4239–4261.

Regehr, W. G., Connor, J. A., and Tank, D. W. 1989. Optical imaging of calcium accumulation in hippocampal pyramidal cells during synaptic activation. *Nature (London)* **341**, 533–536.

Santos, R. M., Rosario, L. M., Nadal, A., Garcia-Sancho, J., Soria, B., and Valdeolmillos, M. 1991. Widespread synchronous $[Ca^{2+}]_i$ oscillations due to bursting electrical activity in single pancreatic islets. *Pflugers Arch.* **418**, 417–422.

Sernagor, E., and Grzywacz, N. M. 1993a. Cellular mechanisms underlying spontaneous correlated activity in the turtle embryonic retina. *Invest. Ophthalmol. Vis. Sci.* **34**, 1156.

Sernagor, E., and Grzywacz, N. M. 1993b. Emergence of isotropic and anisotropic receptive-field properties in the developing turtle retina. *Neurosci. Abst.* **19**, 53.

Sernagor, E., and Grzywacz, N. M. 1994. Synaptic connections involved in

the spontaneous correlated bursts in the developing turtle retina. *Invest. Opthalmol. Vis. Sci.* **35**, 2125.

Sherman, A., and Rinzel, J. 1991. Model for synchronization of pancreatic β-cells by gap junction coupling. *Biophys. J.* **59**, 547–559.

Skaliora, I., Scobey, R. P., and Chalupa, L. M. 1993. Prenatal development of excitability in cat retinal ganglion cells: Action potentials and sodium currents. *J. Neurosci.* **13**, 313–323.

Somjen, G. G. 1979. Extracellular potassium in the mammalian central nervous system. *Annu. Rev. Physiol.* **41**, 159–177.

Van Harreveld, A. 1972. The extracellular space in the vertebrate central nervous system. In *The Structure and Function of Nervous Tissue*, G. H. Bourne, ed., pp. 447–511. Academic, New York.

Winfree, A. T. 1990. Vortex action potential in normal ventricular muscle. *Ann. N. Y. Acad. Sci.* **591**, 190–207.

Winslow, R. L., Kimball, A. L., Varghese, A., and Noble, D. 1993. Simulating cardiac sinus and atrial network dynamics on the Connection Machine. *Physica D* **64**, 281–298.

Wong, R. O. L., Chernjavsky, A., Smith, S. J., and Shatz, C. J. 1992. Correlated spontaneous calcium bursting in the developing retina. *Neurosci. Abstr.* **18**, 923.

Wong, R. O. L., Meister, M., and Shatz, C. J. 1993. Transient period of correlated bursting activity during development of the mammalian retina. *Neuron* **11**, 923–938.

Yamada, W. M., Koch, C., and Adams, P. R. 1989. Multiple channels and calcium dynamics. In *Methods in Neuronal Modeling*, C. Koch and I. Segev, eds., pp. 97–133. MIT Press, Cambridge, MA.

Zucker, C., and Yazulla, S. 1982. Localization of synaptic and nonsynaptic nicotinic-acetylcholine receptors in the goldfish retina. *J. Comp. Neurol.* **204**, 188–195.

Received September 3, 1993; accepted January 11, 1994.